ARTICLE NO. 79-0890R

A80-080

Technology and Operational Considerations for Low-Heat-Rate Entry Trajectories

40001
70012

Kathryn E. Wurster* and Charles H. Eldred†
NASA Langley Research Center, Hampton, Va.

A broad parametric study which examines several critical aspects of low-heat-rate entry trajectories is performed. Low planform loadings associated with future winged Earth-entry vehicles coupled with the potential application of metallic thermal protection systems suggest that such trajectories are of particular interest. Some aspects of these trajectories included in this study are: three heating conditions, i.e., reference, stagnation, and windward centerline (for both laminar and turbulent flow); configuration-related factors including planform loading and hypersonic angle of attack; and mission-related factors such as crossrange and orbit inclination. Results indicate benefits in the design of thermal protection systems are to be gained by utilizing moderate angles of attack, as opposed to high lift coefficients coupled with high angles of attack, during entry. An assessment of design and technology implications is made.

Nomenclature

c.g.	= center of gravity in percent of body reference length measured from the disappearing apex of the nose
C_L	= lift coefficient
c_p	= specific heat at constant pressure, J/kg·K
L/D	= lift-to-drag ratio
M	= Mach number
$\dot{q}$	= heat rate, kW/m^2
$\dot{q}_{ref}$	= reference heat rate, kW/m^2
Re_θ	= momentum thickness Reynolds number
S	= reference area, m^2
W	= weight, kN
W/C_LS	= lift-loading coefficient, kN/m^2
α	= angle of attack, deg
ρ	= density, kg/m^3

Introduction

THE technical community is rapidly becoming aware of the vast potential which exists for the utilization of space, especially in the near-Earth-orbit region. The space shuttle and its projected heavy-lift derivatives represent the first step toward reduced space transportation costs and improved capability necessary to attract users. Even further advancements in these directions will be required before truly large-scale space operations and the industrialization of space can become a reality. Any new space transportation system must provide the necessary gain in capability and yet reduce space transportation costs substantially enough to stimulate new commerical uses of space.

Winged entry vehicle concepts of the 1950's and 1960's were characteristically small and relatively dense vehicles. These factors, along with the existing high-temperature materials technology, combined to make the stagnation areas the primary concern of the thermal protection system (TPS) design. This led to the interest in high-C_L (high-α) entry trajectories as a means of alleviating stagnation temperatures and heating rates. Concepts for future winged entry vehicles are characteristically considerably larger (larger leading-edge radii at stagnation conditions), have lower planform loadings, and have space-shuttle-type stagnation materials. Consequently, the TPS concerns will focus more on the non-stagnation areas of the windward body and wing surfaces. High-lift trajectories will not necessarily be the choice for these vehicles.

As presently envisioned, a new space transportation system will include a second-generation winged Earth-entry vehicle. The TPS is a very sizable cost item on any winged Earth-entry vehicle, and, consequently, this area has potential for substantial cost reduction. The present shuttle vehicle utilizes a reusable surface insulation (RSI). This type of TPS is particularly well suited to the shuttle mission, since an RSI allows a TPS of a relatively simple design, its thermal properties are well characterized, and heat transfer through this type of TPS is well understood. The RSI is capable of withstanding high temperatures [1530 K (2300°F)], and a one-time over-temperature will not result in a catastrophic failure.

Many uncertainties exist in the area of heating for winged entry vehicles. Very little flight-test data, which could be used to substantiate heating theories in the hypersonic flight regime, are available for such configurations. Because of the large heating uncertainties which exist for the shuttle, the over-temperature capability of the RSI is of particular importance, especially from a crew-safety and vehicle-reusability point of view. However, one important problem area for RSI is its long-term serviceability. The relatively fragile nature of the RSI materials and the current labor-intensive refurbishment techniques may turn out to be obstacles to achieving the low TPS maintenance costs desired for future vehicles. Metallic TPS's (including both hot structures and standoff systems), because of their more rugged material properties, have the potential to achieve goals of low operational costs for future Earth-entry vehicles.

The TPS requires an integrated design effort at the vehicle system level. In addition to the economic aspects mentioned previously, vehicle configuration characteristics, mission factors, TPS materials, and detail design will all be important considerations for future TPS's. The entry trajectory can be a powerful tool for winged vehicle design because such vehicles normally have considerable latitude in shaping the entry flight to TPS considerations. One of the key considerations is the peak heating rate and the associated external surface temperatures. For metallic TPS's, low-heat-rate entry trajectories

Presented as Paper 79-0890 at the AIAA/NASA Conference on Advanced Technology for Future Space Systems, Hampton, Va., May 8-11, 1979; submitted July 17, 1979; revision received March 31, 1980.

Index categories: Entry Vehicle Mission Studies and Flight Mechanics; LV/M Aerodynamic Heating and Ablation.

*Aerospace Engineer, Vehicle Analysis Branch, SSD. Member AIAA.

†Assistant Head, Vehicle Analysis Branch, SSD. Member AIAA.

are of particular interest because fairly large weight savings can be realized with the associated temperature decreases. Future vehicles are expected to have significantly lower planform loadings than the space shuttle orbiter, thus improving the potential for low-heat-rate entries. Specially tailored trajectories will be necessary to realize the full potential of the metallic-class TPS's. The purpose of this study is to define the potential for low-heat-rate entry trajectories for future systems and to identify associated technology requirements.

A broad parametric study which includes: three heating conditions, i.e., reference heating, stagnation-area heating, and windward-centerline heating (both laminar and turbulent); configuration-related factors including planform loading and hypersonic angle of attack; and mission-related factors such as crossrange and orbit inclination, is discussed herein. Detailed heating analyses are performed using the aerodynamic heating program MINIVER,[1] and optimized entry trajectories are generated using the POST (Program to Optimize Simulated Trajectories) computer program.[2] Design and technology implications are also discussed.

Vehicle Description

A control-configured-vehicle (CCV) concept[3] was used as a representative Earth-to-orbit vehicle in the present study. The reference vehicle, shown in Fig. 1, is a fully reusable, delta-wing, vertical-takeoff, horizontal-landing, single-stage-to-orbit (SSTO) vehicle. The following vehicle characteristics at entry were used: weight, 1.9 MN (430,000 lb); reference wing area, 557.4 m^2 (6000 ft^2); vehicle length, 66.8 m (219 ft); and planform loading, 1.7 kN/m^2 (35.5 lb/ft^2). Experimental aerodynamic characteristics of the reference vehicle[4,5] were used. Maximum C_L for hypersonic velocities occurs at a 50-deg angle of attack. Hypersonic L/D_{max} occurs at approximately a 15-deg angle of attack with a value of about 2.1.

Method of Analysis

MINIVER

Detailed heating analyses were performed using the MINIVER aerodynamic heating program. Trajectory inputs included altitude, velocity, and angle-of-attack time histories. The 1962 U.S. standard atmosphere properties[6] were used in the heating analyses. The flow over the lower surface of the reference vehicle was modeled using a delta-wing configuration with a crossflow technique which accounts for the effects of local flow divergence at angle of attack.[7] The TPS characteristics employed were those of a metallic TPS applicable to reentry vehicles. This TPS consisted of a corrugation-stiffened skin fabricated from L-605, a cobalt-base superalloy similar to Haynes 188.[8] The MINIVER surface model used was a thin skin (infinite conductivity), 0.063-cm (0.025 in.) thick, with L-605 material properties (ρ, c_p) and an emissivity of 0.8. The initial skin temperature chosen was 311 K (100°F), a value shown in previous studies to be consistent with typical vehicle attitude, orbital inclinations, and thermal control on orbit.[9]

The analytical heating methods employed in MINIVER were varied depending on the particular heating condition under consideration. Stagnation point heating was evaluated using the well-known Fay and Riddell stagnation point method.[10] Laminar heating along the windward centerline was calculated using the Eckert reference enthalpy flat plate method,[11] and turbulent heating was analyzed using the Spalding and Chi flat plate method.[12] The transition criteria employed were based upon the momentum thickness Reynolds number Re_θ and the local Mach number M. Transition onset was assumed at a value of $Re_\theta/M=225$, and fully turbulent flow was assumed at $Re_\theta/M=265$, consistent with space shuttle transition criteria.

POST

Trajectories were generated by the POST program using a planet model for a spherical rotating Earth. The form of the 1962 standard atmosphere used in this portion of the analysis assumes a constant molecular weight above an altitude of 90 km.[2] Initial entry conditions at 122 km (400,000 ft) were determined by deorbit from a 185.2-km (100 n.mi.) orbit with a slightly retrograde inclination to yield the maximum crossrange. The initial latitude and longitude were 47.8°N and 17.2°E; the inertial velocity, heading, and flight-path angle were 7818 m/s (25,600 ft/s), 339, and −0.84 deg, respectively. The following description is characteristic of all the entry trajectories generated in this study. Each employed a two-step angle-of-attack profile with a relatively high angle at hypersonic speeds held constant to 2440 m/s (8000 ft/s), followed by a pitch down to 12 deg at 1070 m/s (3500 ft/s). Entries were generally initiated with a nonzero bank angle so that maximum utilization of the turning capability at hypersonic Mach numbers could be made. The bank angle was modulated, increasing and decreasing lift as necessary, to maintain the peak reference-heat-rate limit. In this way, a minimal heat load for a given peak heat rate was achieved. Acceptable peak heat rates were determined by material temperature constraints. After the high heating phase of the entry, the bank angle was decreased to zero degrees.

Heating rates are determined in POST by a simplified heating analysis based on Chapman's equation for stagnation point heating to a sphere.[13] Reference values based on a 0.305-m (1 ft) radius sphere were used for comparison purposes. Chapman's equation gives reference heat rates as a function of altitude and relative velocity. Heat load was simply calculated as the stagnation heat rate integrated over the time of the trajectory. Crossrange calculations were computed relative to the ground track of the reference circular orbit and represent one-half the footprint of the entering vehicle. Crossrange values quoted are those achieved at the end of the entries (altitude = 0).

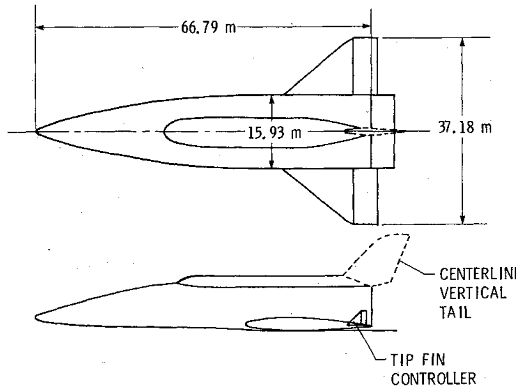

Fig. 1 Line drawing of control-configured vehicle used in study.

Results and Discussion

Minimum Heat-Rate Limits

Winged entry vehicles typically have the aerodynamic capability to fly entry trajectories within a broad altitude-velocity envelope. The upper boundary of this envelope is an aerodynamic limit associated with equilibrium glide at zero bank angle. Equilibrium glide altitude-velocity profiles for entry from a polar orbit are shown in Fig. 2 for different values of the lift-loading coefficient W/C_LS. Figure 3 illustrates a family of reference-heat-rate contours as defined by Chapman's equation. The altitude-velocity values for an equilibrium glide trajectory for a lift-loading coefficient typical of the reference vehicle are superimposed on these reference-heat-rate contours in Fig. 4. The reference heat rate varies along an equilibrium glide path with the peak heat rate

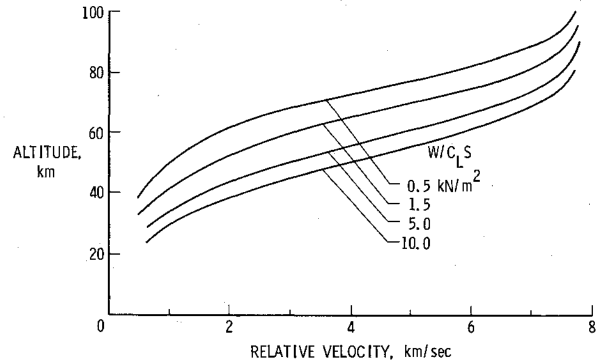

Fig. 2 Equilibrium glide capability; polar inclination, zero bank angle.

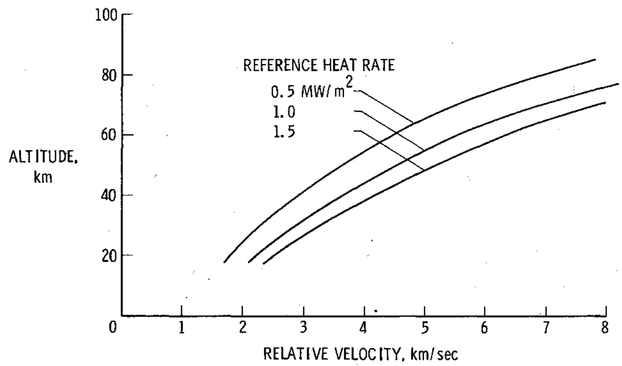

Fig. 3 Reference-heat-rate contours; Chapman's equation, reference sphere radius = 0.305 m.

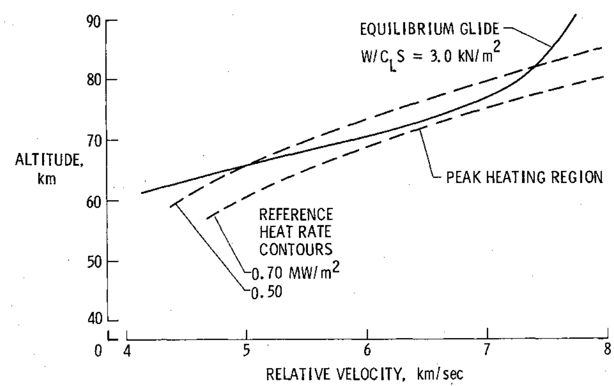

Fig. 4 Reference heating characteristics along a representative equilibrium glide trajectory; polar inclination.

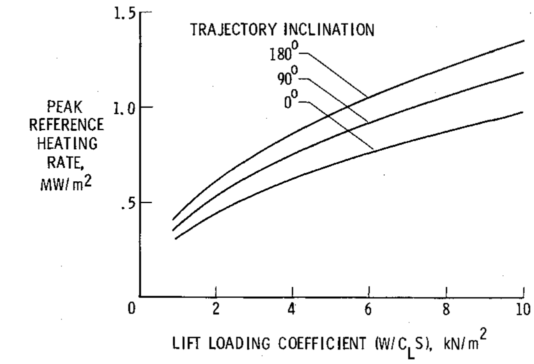

Fig. 5 Peak reference heating rate along equilibrium glide trajectories; relative velocity ≃ 6500 m/s.

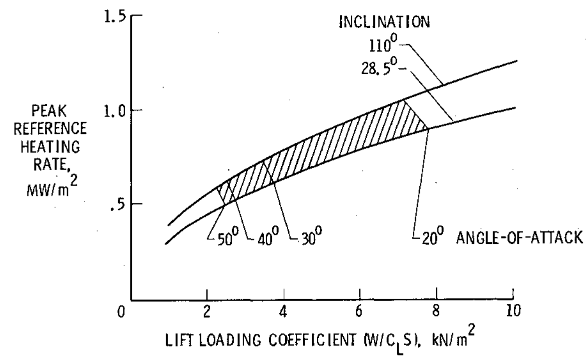

Fig. 6 Minimum reference heating envelope for a typical SSTO advanced winged CCV.

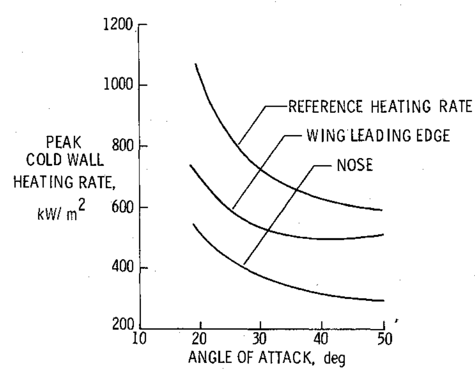

Fig. 7 Angle-of-attack effects on peak stagnation heating for equilibrium glide trajectories; polar inclination, CCV.

occurring for an Earth-relative velocity of approximately 6500 m/s (21,400 ft/s). As shown in the previous figures, the minimum peak-reference-heat-rate value which can be achieved increases with increasing value of the parameter $W/C_L S$.

Peak heating generally occurs well after the initial pullout of the typical entry trajectory at a speed where centrifugal lift still exerts a strong influence on the equilibrium glide trajectory. Consequently, the velocity direction relative to the Earth's rotation has a significant impact on the value of the peak reference heat rate. Figure 5 shows the critical peak reference heat rate as a function of $W/C_L S$ and initial orbit inclination, and illustrates the minimum achievable peak reference heat rate for a given orbit inclination and lift-loading coefficient. The minimum peak reference heat rate for a due-east mission (0-deg inclination) is significantly lower than that for a due-west mission (180 deg). The extremes of due east and due west are, however, not expected to be of practical concern. Presently anticipated missions generally require orbital inclinations between 110 and 28.5 deg. This figure can easily be used for a sensitivity assessment of a number of the factors which influence entry heating: entry weight, wing area, planform loading, lift coefficient, and mission inclination. For the range of inclinations of interest, Fig. 6 shows an envelope of the peak reference heating rate as a function of $W/C_L S$ for the reference vehicle. Lines of constant angle of attack are shown to be inclined due to the difference in payload capability for east and polar entries [29,500 kg (65,000 lb) for east entry, and 18,150 kg (40,000 lb) for west]. These figures show that a significant reduction in peak reference heat rate occurs with increased angle of attack (due to increased lift coefficient at higher angles of attack). Figure 7 illustrates the close relationship between the nose and wing stagnation heating and the reference heat rate when bow shock/wing shock interaction is not a factor. The reference heat rate appears to be a good indicator of stagnation heating.

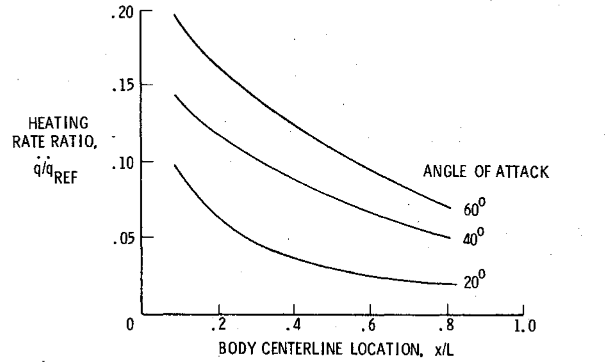

Fig. 8 Angle-of-attack effects on nondimensional windward-centerline laminar heating.

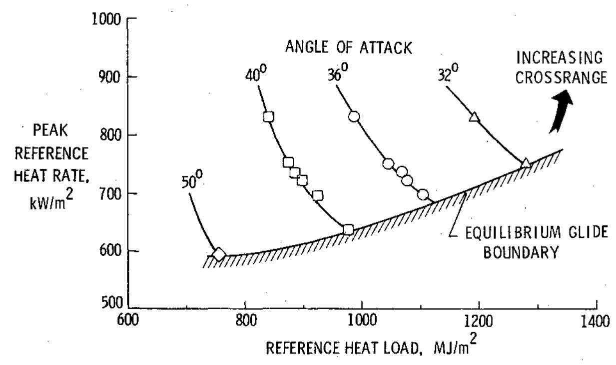

Fig. 10 Heat-load effects for low-heat-rate trajectories optimized for maximum crossrange; CCV.

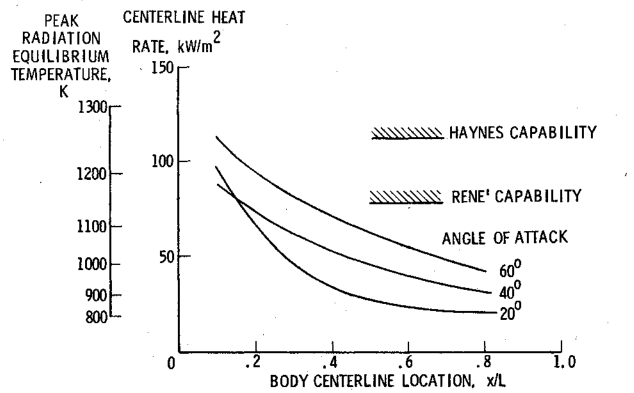

Fig. 9 Angle-of-attack effects on peak windward-centerline heating along an equilibrium glide trajectory; polar inclination, laminar, CCV.

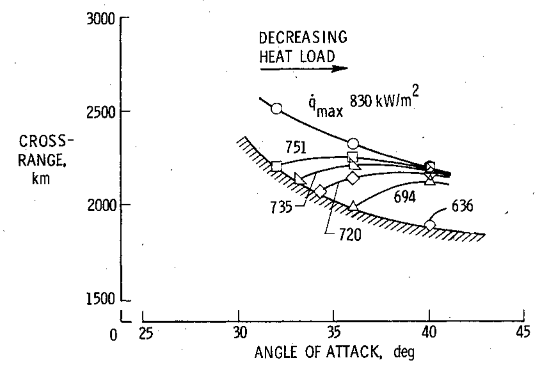

Fig. 11 Crossrange for low-heat-rate trajectories; laminar heating only.

Although much can be inferred from these charts regarding stagnation-area heating, windward-surface heating requires additional analysis.

Angle-of-attack effects on typical laminar, nondimensional, windward-centerline heating distributions[14] are shown in Fig. 8. Although there was a large reduction in reference-heat-rate values at high angles of attack, windward-centerline heat rates show the opposite trend. The combined effects of C_L and α on the centerline heating rates for the reference vehicle are shown in Fig. 9. The heat-rate values shown are the peak values which occur along an equilibrium glide trajectory on entry from a polar orbit. Lower angles of attack appear to relieve the laminar windward heating rates (aft of a body centerline location of about 0.15) despite the higher stagnation-area heating rates associated with the lower angles. In the past, the primary concern was the protection of the vehicle in the high-heating stagnation regions. High angle-of-attack entries were dictated by the necessity to limit the heating rates in the stagnation regions to values within the temperature capabilities of the existing stagnation materials. Development of high-temperature stagnation materials during the shuttle program now allows a trade to be made between the stagnation-area heating and the windward-surface heating. Compared to the stagnation area, the windward surface represents a much larger portion of the vehicle; therefore, reducing the heating over this area offers the potential for more significant benefits. Shown also in Fig. 9 are the temperature capabilities of two candidate metallic TPS materials, Haynes 188 and René 41. The indicated trade would favor utilization of a lower angle of attack to limit the majority of the lower surface to less than the 1255 K (1800°F) temperature capability of the Haynes system. This could necessitate the use of a hybrid TPS employing advanced RSI or carbon-carbon in the high-temperature stagnation areas and a metallic system for the remainder of the lower surface.

Reduction in angle of attack must be limited, however, so that the stagnation heat rates do not exceed the temperature capabilities of the stagnation TPS material. An angle of attack of ~30 deg would probably satisfy these requirements. A number of problem areas must be dealt with, however, when considering utilization of lower angles of attack for winged vehicles on entry. These include hypersonic angle-of-attack trim requirements, bow shock/wing shock interaction, and angle-of-attack impact on turbulent heating. Each of these areas must be examined in greater detail and will be discussed in a later section.

Impact of Operational Requirements

Equilibrium glide is not the normal choice for an entry trajectory; however, the critical heating point on an equilibrium glide is also a critical or limiting condition for any entry trajectory. For reasons of minimizing the heat load and also of generating a turn to give crossrange, bank-angle control is normally used to fly along a constant heat-rate boundary. The minimum heat-rate trajectory will have zero bank at the critical heating point (around 6500 m/s relative velocity); however, in relation to that critical heat rate, the vehicle has excess lift capability both before and after that point, allowing banking maneuvers to be performed without exceeding the critical heat rate.

Optimized entry trajectories of this type have been used to determine crossrange and heat-load effects. The baseline configuration entering from a polar orbit was used in POST to generate maximum crossrange trajectories subject to peak reference-heat-rate constraints. Figure 10 indicates heat-load trends and shows the typical tradeoff between heat rate and heat load for each angle of attack. Reduction in the allowable reference heat rate for a given angle of attack results in a penalty in the total heat load which must be accommodated; the greater the lift-curve slope, the larger the penalty. This plot also demonstrates the expected trend toward lower stagnation heat load at higher angles of attack for a given heat rate. The lower curve represents minimum peak-heat-rate, equilibrium glide values. Restriction to low stagnation heat rates necessarily limits the minimum value of angle of attack which may be used.

A summary of the results of this portion of the study is presented in Fig. 11 where crossrange is plotted as a function of hypersonic angle of attack and peak reference heat rate for the same trajectories. The lower left boundary corresponds to the equilibrium glide boundary in the previous figure and represents minimum heat-rate trajectories for the given angles of attack. The crossrange value corresponding to this boundary is "free" to the extent that no heat-rate penalty is associated with that crossrange. For a given α, this chart indicates the additional crossrange that can be realized by relaxing the peak-heat-rate constraint. Along the minimum heat-rate boundary and at the higher heat rates ($\dot{q}_{ref} \geq \sim 830$ kW/m^2), crossrange increases with decreasing angle of attack; that is, the conventional association of crossrange capability with L/D (increased L/D yields increased crossrange). However, at lower constant-heat-rate boundaries ($\dot{q}_{ref} \leq \sim 751$ kW/m^2), crossrange increases with increasing angle of attack. In this case, the increase in lift coefficient allows for more turning capability (higher bank angles). For moderate angles of attack (30-40 deg) and crossranges in the neighborhood of 2000-2200 km (in the low-heat-rate region), decreases in angle of attack for a given crossrange will increase the stagnation heat rate. As discussed previously, though, decreases in angle of attack will generally lessen the severity of heating along the windward side. Thus, for the low-heat-rate trajectories of interest here, the lowest angle of attack required to achieve the necessary crossrange should be used. The corresponding mild increases in stagnation-area heating should be acceptable for a vehicle utilizing these low-heat-rate trajectories. However, for high crossranges, greater than 2400 km (in the higher heat-rate region), decreases in angle of attack for a given crossrange will decrease stagnation heating. Results discussed in the previous section indicate that decreased stagnation heating does not necessarily lead to reduced body heating. An analysis of windward heating rates for a range of angles of attack at constant crossrange (such as indicated in Fig. 11) leads to a conclusion similar to the one from the previous section, that is, low surface temperatures are related to reduced angle of attack. Figure 11 also shows that 2037 km (1100 n.mi.) of crossrange (required for a single-pass return capability) are readily available for all but the very low-heat-rate cases. This indicates that crossrange may present a problem in the case of metallic TPS's with very low-temperature constraints.

Technology Implications of Low-α Entries

Several problems come to mind immediately when considering utilization of lower hypersonic angles of attack for winged vehicles on entry. The first of these is trim requirements at hypersonic angles of attack. These vehicles typically have far-aft c.g. locations ($\sim$73% for the reference vehicle). Trim requirements will undoubtedly impose restrictions on acceptable α values. Figure 12 indicates the angle-of-attack trim boundaries for the reference vehicle with a c.g. location at 73% of the body length. A typical low-α entry trajectory profile is also shown. The "corner" at Mach 5 is the only problem immediately evident for these trajectories. The lower angle of attack actually appears to relieve this problem. For higher angles of attack, the trajectory could easily be tailored to the trim limits with negligible, if any, effects on the heating. A second possible problem at lower entry α is that of bow shock/wing shock interaction. As the angle of attack is reduced at hypersonic Mach numbers, the bow shock moves in toward the body and may impinge on the wing, resulting in an area of extremely high heating. Electron-beam photographs of the reference vehicle, taken during tests at Mach 20 in helium for various angles of attack, indicate

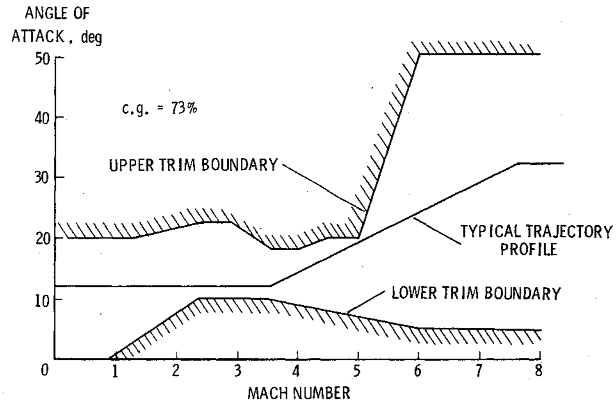

Fig. 12 Angle-of-attack trim boundaries; CCV.

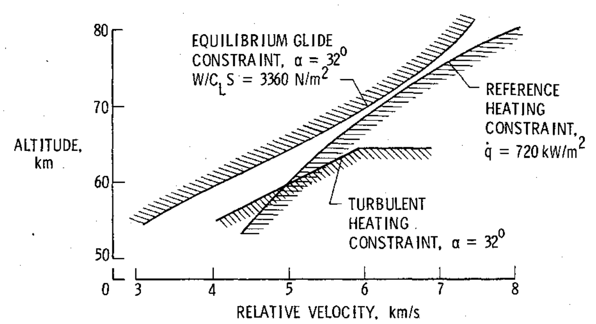

Fig. 13 Entry trajectory corridor for heating constraints on a typical SSTO advanced winged vehicle; polar inclination.

that the fineness ratio for the reference vehicle is sufficiently large so that bow shock/wing shock interference, even at angles of attack down to 30 deg, is avoided. This evidence is, however, not conclusive because of the relatively low normal-shock-density ratio for helium.

Future winged entry vehicles will be significantly larger than the present shuttle vehicle, increasing the likelihood that turbulent heating will occur over a sizable portion of the vehicle. A great deal of uncertainty exists in the area of turbulent heating and the criteria which should be used to predict transition onset. The effects of angle of attack on transition for winged-entry-type vehicles are still largely unknown. Using $Re_\theta/M=265$ to define the location of fully turbulent flow, the effects of turbulent heating were examined for two angle-of-attack entry cases, 40 and 32 deg. Figure 13 illustrates an entry corridor which could be flown for a 32-deg entry to reduce the impact of turbulent heating on the TPS design. The upper boundary represents an equilibrium glide trajectory for a typical lift-loading coefficient. A reference-heat-rate contour which would limit the stagnation temperature to an appropriate value for the material chosen (advanced RSI or carbon-carbon) forms the lower-right boundary of the corridor. The horizontal line represents the altitude at which transition will occur at 60 m, the aft end of the vehicle. This boundary should not be crossed until velocities are low enough to limit turbulent heat rates to values within the capability of the metallic TPS. In this case, the René 41 capability of 1144 K (1600°F) is used as the maximum temperature limit (shown as the turbulent heating constraint). A typical trajectory might follow the reference-heat-rate limit until transition altitude is reached. This altitude would be maintained until velocities are sufficiently low so that turbulent heating would not exceed the limit of the TPS material. An altitude-velocity line of constant turbulent heat rate (constant temperature, turbulent heating boundary) could then be followed through the high-heating phase of the trajectory.

The same boundaries were also determined for the $\alpha = 40$-deg case. They appeared to be remarkably similar to the $\alpha = 32$-deg case, with the major difference being that the transition altitude and lines of constant turbulent heat rate are shifted up about 3000 m in altitude. A trajectory similar to that previously described could also be flown for the higher angle-of-attack case. These results seem to indicate that TPS requirements need not be impacted greatly by turbulent heating effects at lower angles of attack. However, the choice of transition criteria could impact these results significantly. Transition is expected to vary with angle of attack, although precisely how is uncertain. Flight-test data from the shuttle may give a better understanding of the onset of transition and turbulent heating. Turbulent heating, bow shock/wing shock interaction, and hypersonic trim problems each need to be examined in greater detail before entry strategy recommendations involving low angles of attack can be made with real confidence.

Conclusions

The following may be concluded from this study:

1) Orbit inclination is an important design consideration for low-heat-rate thermal protection systems (TPS's).

2) The reference heat rate is not a good indicator for windward-surface heat rates when angle-of-attack variations are considered.

3) Low windward-surface temperatures require relatively low angles of attack, but stagnation temperatures tend to limit the value of these angles. Thirty degrees may be a reasonable value which limits stagnation temperatures to less than 1922 K (3000°F), and most of the lower surface to less than 1255 K (1800°F). This could result in a hybrid TPS requiring advanced reusable surface insulation (RSI) or carbon-carbon in the hot stagnation areas and a metallic TPS for the lower surface.

4) For this range of low α (~ 30 deg), a well over 2200 km (1200 n.mi.) of crossrange is available at no heat-rate penalty.

5) For high-heat-rate trajectories, decreased α (increased L/D) increases crossrange for a given heat-rate constraint, as expected. However, for low-heat-rate trajectories at moderate angles of attack, increased α increases crossrange for a given heat-rate constraint.

6) Turbulent heating appears to have essentially the same impact on TPS design at moderate angles of attack (32-40 deg). Much uncertainty still exists in the area of turbulent heating, however, and a more detailed understanding of transition on large winged entry vehicles is necessary before entry strategy recommendations involving low α can be made with real confidence.

In working toward a goal of low operational costs for future space transportation systems, metallic TPS's on low-planform-loaded winged vehicles which fly low-heat-rate trajectories may be a viable option. Low hypersonic angles of attack may be an important step toward use of metallic systems, but more detailed study, especially in the area of transition and turbulent heating, is necessary before the question of low or high hypersonic angle of attack can be resolved.

References

[1] Hender, D.R., "A Miniature Version of the JA-70 Aerodynamic Heating Computer Program, H800 (MINIVER)," McDonnell Douglas Astronautics Co., Huntington Beach, Calif., MDC Report G0462, June 1970 (revised Jan. 1972).

[2] Brauer, G.L., Cornick, D.E., and Stevenson, R., "Capabilities and Applications of the Program to Optimize Simulated Trajectories (POST)," NASA CR-2770, Feb. 1977.

[3] Freeman, D.C., Jr. and Powell, R.W., "The Results of Far-Aft Center-of-Gravity Location on the Design of a Single-Stage-to-Orbit Vehicle System," AIAA Paper 79-0892, AIAA/NASA Conference on Advanced Technology for Future Space Systems, Hampton, Va., May 8-11, 1979.

[4] Bernot, P.T., "Aerodynamic Characteristics of Two Single-Stage-to-Orbit Vehicles at Mach 20.3," NASA TM X-3550, Aug. 1977.

[5] Freeman, D.C., Jr. and Wilhite, A.W., "Effects of Relaxed Static Longitudinal Stability on a Single-Stage-to-Orbit Vehicle Design," NASA TP-1594, Dec. 1979.

[6] *U.S. Standard Atmosphere, 1962*, NASA, U.S. Air Force, and U.S. Weather Bureau, Dec. 1962.

[7] Baranowski, L.C., "Influence of Crossflow on Windward-Centerline Heating," McDonnell Douglas Corp., St. Louis, Mo., MDC Report E0535, Dec. 1971.

[8] Sawyer, J.W., "Aerothermal and Structural Performance of a Cobalt-Base Superalloy Thermal Protection System at Mach 6.6," NASA TN D-8415, May 1977.

[9] Masek, R.V., Hender, D.R., and Forney, J.A., "Evaluation of Aerodynamic Heating Uncertainties for Space Shuttle," *Journal of Spacecraft and Rockets,* Vol. 2, June 1974, pp. 368-375.

[10] Fay, J.A. and Riddell, F.R., "Stagnation Point Heat Transfer in Dissociated Air," *Journal of the Aeronautical Sciences,* Vol. 25, No. 2, 1958, pp. 73-85, 121.

[11] Eckert, E.R.G., "Survey of Boundary-Layer Heat Transfer at High Velocities and High Temperatures," Wright Air Development Center, Dayton, Ohio, WADC Technical Report 59-624, April 1960.

[12] Spalding, D.B. and Chi, S.W., "The Drag of a Compressible Turbulent Boundary Layer on a Smooth Flat Plate with and without Heat Transfer," *Journal of Fluid Mechanics,* Vol. 18, Pt. 1, Jan. 1964, pp. 117-143.

[13] Chapman, D.R., "An Approximate Analytical Method for Studying Entry into Planetary Atmospheres," NASA TR R-11, 1959.

[14] Matthews, R.K., Buchanan, T.D., Martindale, W.R., and Warmbrod, J.D., "Experimental and Theoretical Aerodynamic Heating and Flowfield Analysis of a Space Shuttle Orbiter," Vol. II, NASA TMX-2507, Feb. 1972.